MID-AMERICA TRANSPORTATION CENTER

Report # MATC-MS&T: 132-2

Final Report
WBS: 25-1121-0005-132-2

SMART Shear Keys for Multi-Hazards Mitigation of Diaphragm-Free Girder Bridges - Phase II: Numerical Simulation on Seismic Performance

Genda Chen, PhD, PE
Professor and Robert W. Abbett Distinguished Chair in Civil Engineering
Department of Civil, Architectural, and Environmental Engineering
Missouri University of Science and Technology

Haibin Zhang, PhD
Research Consultant

Xinzhe Yuan
PhD Candidate

Tarutal Ghosh Mondal, PhD
Postdoctoral Fellow

2022

A Cooperative Research Project sponsored by
U.S. Department of Transportation- Office of the Assistant Secretary for Research and Technology

SMART Shear Keys for Multi-Hazards Mitigation of Diaphragm-Free Girder Bridges – Phase II: Numerical Simulation on Seismic Performance

Haibin Zhang, Ph.D.
Research Consultant
Department of Civil, Architectural, and Environmental Engineering
Missouri University of Science and Technology

Xinzhe Yuan, Ph.D. Candidate
Department of Civil, Architectural, and Environmental Engineering
Missouri University of Science and Technology

Tarutal Ghosh Mondal, Ph.D.
Postdoctoral Fellow
Department of Civil, Architectural, and Environmental Engineering
Missouri University of Science and Technology

Genda Chen, Ph.D., P.E.
Professor and Robert W. Abbett Distinguished Chair in Civil Engineering
Department of Civil, Architectural, and Environmental Engineering
Missouri University of Science and Technology

A Report on Research Sponsored by

Mid-America Transportation Center

University of Nebraska–Lincoln

July 6, 2022

Technical Report Documentation Page

1. Report No. 25-1121-0005-132-2	2. Government Accession No.	3. Recipient's Catalog No.
4. Title and Subtitle SMART Shear Keys for Multi-Hazards Mitigation of Diaphragm-Free Girder Bridges - Phase II: Numerical Simulation on Seismic Performance		5. Report Date July 6, 2022
		6. Performing Organization Code
7. Author(s) Haibin Zhang, Xinzhe Yuan, Tarutal Ghosh Mondal, and Genda Chen		8. Performing Organization Report No. 25-1121-0005-132-2
9. Performing Organization Name and Address Center for Intelligent Infrastructure Department of Civil, Architectural, and Environmental Engineering Missouri University of Science and Technology 500 W. 16th St. Rolla, MO 65409-0810		10. Work Unit No. (TRAIS)
		11. Contract or Grant No. 69A3551747107
12. Sponsoring Agency Name and Address Office of the Assistant Secretary for Research and Technology 1200 New Jersey Ave., SE Washington, D.C. 20590		13. Type of Report and Period Covered Final Report January 1, 2019 – June 30, 2022
		14. Sponsoring Agency Code MATC TRB RiP No. 91994-29
15. Supplementary Notes		

16. Abstract

The observations from past seismic events reveal that the failure of the shear keys caused by inappropriate design leads to an excessive movement or even failure of bridge superstructures. A novel shear key with SMART features, that is Sliding, Modular, Adaptive, Replaceable, and Two-dimensional, is proposed and fabricated to solve this problem. The performance of the SMART shear key is evaluated through experiments. However, only two types of shear keys are experimentally tested with very limited design parameters. Further parametric studies are needed to fully understand the shear keys' performance under various design scenarios. This study aims to conduct a parametric analysis using a numerical simulation method to ascertain the influence of the design parameters of the SMART shear key. In addition, the performance of the SMART shear key under seismic loading will be further investigated in a bridge model. Based on the simulation results, it can be inferred that the SMART shear key is a promising solution for displacement control, optimization of force and displacement balance, and energy dissipation.

17. ORCID No. of each Researcher Haibin Zhang: 0000-0003-4318-8202 Xinzhe Yuan: 0000-0003-4567-5362 Tarutal Ghosh Mondal: 0000-0003-2091-7046 Genda Chen: 0000-0002-0658-4356	18. Distribution Statement		
19. Security Classif. (of this report) Unclassified	20. Security Classif. (of this page) Unclassified	21. No. of Pages 38	22. Price

Table of Contents

List of Figures

List of Tables

Acknowledgments

The authors would like to thank Dr. Jian Zhong for his help in the OpenSEES modeling.

Disclaimer

The contents of this report reflect the views of the authors, who are responsible for the facts and the accuracy of the information presented herein. This document is disseminated in the interest of information exchange. The report is funded, partially or entirely, by a grant from the U.S. Department of Transportation's University Transportation Centers Program. However, the U.S. Government assumes no liability for the contents or use thereof.

Executive Summary

The observations from past seismic events reveal that the failure of the shear keys caused by inappropriate design leads to an excessive movement or even failure of bridge superstructures. A novel shear key with SMART features, that is Sliding, Modular, Adaptive, Replaceable, and Two-dimensional, is proposed and fabricated to solve this problem. The performance of the SMART shear key is evaluated through experiments. However, only two types of shear keys are experimentally tested with very limited design parameters. Further parametric studies are needed to fully understand the shear keys' performance under various design scenarios. This study aims to conduct a parametric analysis using a numerical simulation method to ascertain the influence of the design parameters of the SMART shear key. In addition, the performance of the SMART shear key under seismic loading will be further investigated in a bridge model. Based on the simulation results, it can be inferred that the SMART shear key is a promising solution for displacement control, optimization of force and displacement balance, and energy dissipation.

Chapter 1 Introduction

1.1 Objective

Bridge infrastructure constitutes an essential component of the country's transportation network. However, bridges have been exposed to an increasingly large number of natural hazards, such as earthquakes and tsunamis. The traditional shear keys used in bridges can provide transverse support for the superstructure. However, the damage observed on abutments in the aftermath of the 1994 Northridge Earthquake and 2005 Hurricane Katrina prompted a revision of the shear key design process. Recently, the concept of a Smart shear key that serves as a sacrificial element by inducing sliding shear failure and preventing damage to the abutment stem wall or bent cap has been proposed. If the sacrificial Smart shear keys failed in a seismic event, they could be removed and replaced by a new one for opening up the traffic as soon as possible. Previous studies have explored the basic theory, simulation and experimental behavior of Smart shear key prototypes. However, more detailed investigations are necessary due to the following information gaps which continue to exist. Firstly, the impact of various influencing parameters such as prestress level, friction coefficient and loading path on the performance of the shear key is not clear. Secondly, the energy dissipating capability of shear keys under repeated and monotonic loading has not been thoroughly investigated. Moreover, knowledge is scarce about the performance of shear keys under various seismic loading conditions.

The main objectives of this research program were to develop recommendations for the design of sacrificial shear keys with the intent of determining their peak as well as post-peak responses, to develop design details to reduce damage in the abutment stem walls, and to enable both easy visual inspection and repair of the abutments following a major seismic event.

1.2 Literature review on shear key

1.2.1 Design concept and category

Shear keys are used as sacrificial fuses between the superstructure and substructure to protect the abutment walls, bent cap, and piles from damage by limiting the transverse force that can be transmitted into the abutment. In California, current bridge design specifications (CALTRANS, 2019) state the transverse seismic input forces transferred into the abutment piles are controlled by designing the shear keys such that the maximum shear capacity of the keys does not exceed the smaller of 30% of the dead-load vertical reaction at the abutment and the sum of 75% of the total lateral geotechnical capacity of the piles plus one wing-wall. According to this design approach, it is expected that failure occurs first in the sacrificial shear keys with minimal and repairable damage to the abutment walls. Based on location, shear keys can be divided into two categories, namely exterior shear keys and interior shear keys, as shown in Figure 1.1 and 1.2.

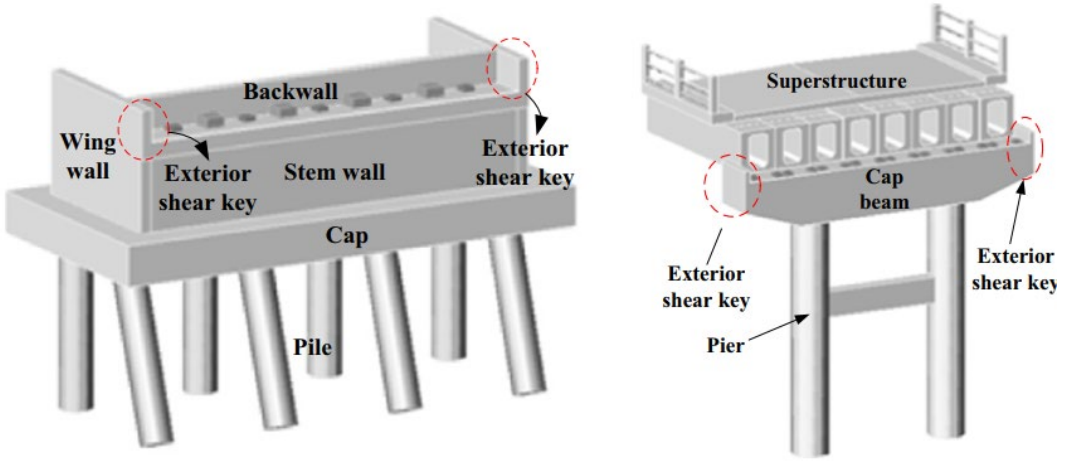

(a) Abutment (b) Cap beam

Figure 1.1 Exterior shear key located at (a) Abutment and (b) Cap beam (Han *et al*., 2017)

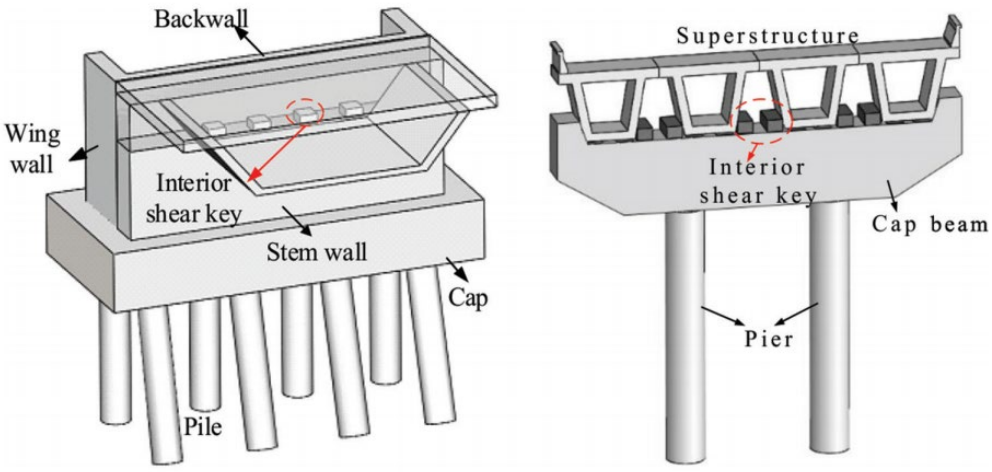

(a) Abutment (b) Cap beam

Figure 1.2 Interior shear key located at (a) Abutment and (b) Cap beam (Han *et al*., 2018)

Based on the difference at the interface of the shear key and abutment/cap beam, it can be categorized into monolithic and isolated shear keys, as shown in Figure 1.3 and 1.4.

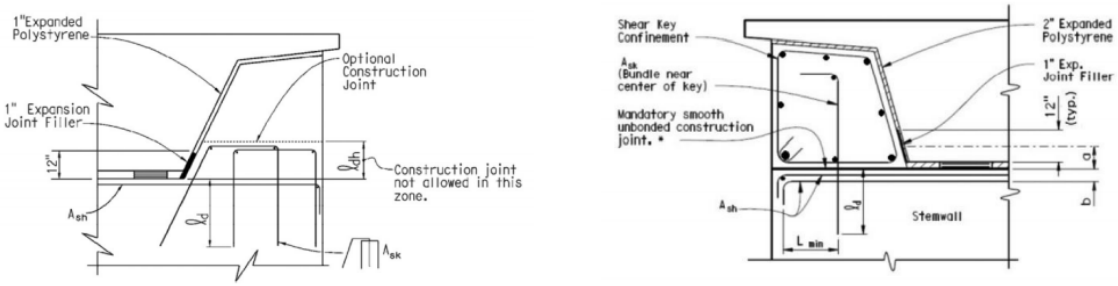

(a) Monolithic shear key (b) Isolated shear key

Figure 1.3 Exterior (a) monolithic and (b) isolated shear key

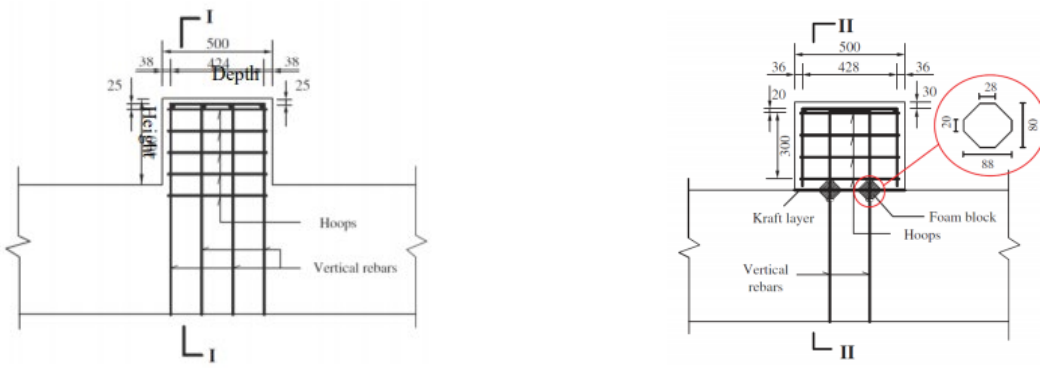

(a) Monolithic shear key (b) Isolated shear key

Figure 1.4 Interior (a) monolithic and (b) isolated shear key

1.2.1.1 Exterior sacrificial shear keys

Megally *et al.* (2001) presented an experimental program to study the seismic response of six exterior sacrificial shear keys. Variables during the test of exterior keys comprised the inclusion of back and wing walls, adoption of different key details, and post-tensioning of the abutment stem wall. Analytical models were developed based on the experimental results. It was found that the shear friction model used in the Caltrans Design Specifications is non-conservative in the design of sacrificial shear keys, which may lead to overloading of the abutments and the supporting piles.

Bozorgzadeh *et al.* (2006) designed and built ten shear keys with different types of connections at the interface of the shear key-abutment and reinforcement at a 1:2.5 scale of a prototype abutment based on Caltrans specifications. The experimental results concluded a smooth construction joint should be used to allow sliding shear failure at the interface of the shear key-abutment stem wall. Additionally, an analytical model was developed for capacity evaluation of exterior shear keys with sliding shear failure.

Silva *et al.* (2009) conducted an experimental performance evaluation of as-built sacrificial exterior shear keys with different construction joint types and load-displacement response at peak and post-peak stages under cyclic loads. Based on the experimental results, a two-spring component hysteretic model with gap and strength degradation was developed, which accurately reproduced the cyclic response of shear keys and their stiffness and capacity degradation caused by the loss of aggregate interlocking and fracture of the reinforcement.

Han *et al.* (2017) presented an experimental study on the seismic behavior of reinforced concrete (RC) sacrificial exterior shear keys, accounting for the influence of reinforcement ratio and construction joint type. Three types of failure modes of the shear key under reversed loads were summarized. Two analytical models for predicting the force-displacement backbone curve were proposed, which were in good agreement with the experimental results.

Kottari *et al.* (2020) proposed a new design method that prevented the sudden unpredictable diagonal shear failure of typical monolithic exterior shear keys, and allowed a more predictable failure mechanism governed by the horizontal sliding of the shear key rather than the diagonal cracking of the stem wall. The analytical formulas and design method were validated by the experimental results.

1.2.1.2 Interior sacrificial shear keys

Megally *et al.* (2001) studied the seismic response of seven interior shear keys. The loading protocol, geometric aspect ratio of the shear key, and reinforcement ratio of the shear key were investigated during the test. Results showed that load history, aspect ratio, and reinforcement ratio have little effect on the response of interior shear keys. However, the aspect ratio affected the degradation of the cyclic friction loading and observed damage levels. A higher aspect ratio led to a lesser degradation of the friction load.

Han *et al.* (2018, 2020) tested the seismic capacity of six interior shear key specimens with different main variables, such as vertical bar number and ratio, hoop ratio, shear span ratio, loading height, and construction joint. Three failure modes of the interior shear key specimens were observed during the tests. Moreover, different analytical models corresponding to the three failure modes and an empirical formula were developed to estimate the seismic capacity of the specimens. When compared with the experimental results, the improved methods provided a more accurate prediction of the load-carrying capacity than the classical analytical models. The interior shear keys with resilient construction joints exhibited satisfactory displacement capacity and limited the damage in the shear keys and cap beams caused by seismic loading.

1.2.2 Failure mode of shear key

1.2.2.1 Diagonal shear failure

This type of failure often happens in monolithic construction joints, which is mainly determined by the total resistance from the vertical reinforcements and hoops crossing the inclined cracks, as shown in Figure 1.5. The failure in the interior shear key happens mainly in the shear key part. For exterior shear keys, however, the cracks propagate diagonally to the toe of the stem wall. The failure mode of exterior shear keys does not entail sacrificial elements, and considerable damage in the abutment can be expected during a major earthquake. Therefore, this failure mode should be avoided for exterior shear keys.

(a) Interior (Han *et al*., 2018)

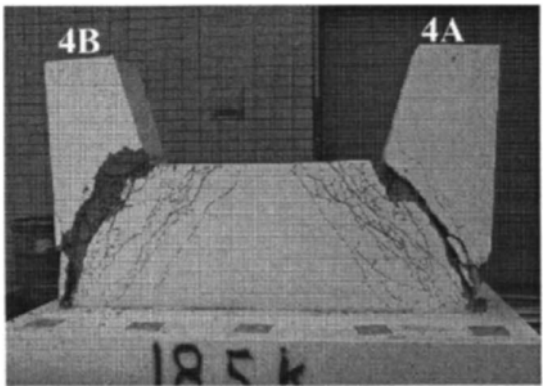

(b) Exterior (Bozorgzadeh *et al*., 2006)

Figure 1.5 Diagonal shear failure mode of shear key

1.2.2.2 Sliding shear failure mode of shear key

The sliding shear failure mode is characterized by the sliding of the shear key at the interface of the shear key–abutment stem wall, followed by concrete spalling and rupture of some vertical shear key reinforcement bars, as shown in Figure 1.6 (a) and (b), respectively.

(a) Interior (Han *et al*., 2018)

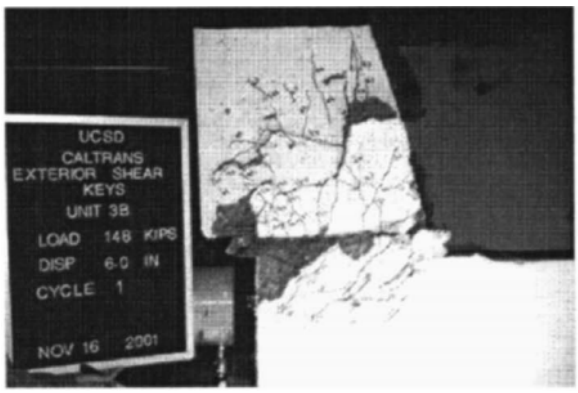

(b) Exterior (Megally *et al*., 2001)

Figure 1.6 Sliding shear failure mode of shear key

1.2.2.3 Shear friction failure

The shear key served as a sacrificial element by inducing sliding shear failure and preventing damage to the abutment stem wall, as presented in Figure 1.7. After reaching the maximum strength, steep softening caused by the breakage of the bond in concrete at the construction joint occurred in this unit. As testing continued in both test units, their capacity gradually increased due to kinking of the shear key vertical reinforcement. At a higher displacement, the shear key vertical reinforcement ruptured, and the shear key failed. The shear keys could be removed, and vertical holes could be drilled so that new vertical reinforcement could be placed; this would be followed by grouting the holes and casting new shear keys.

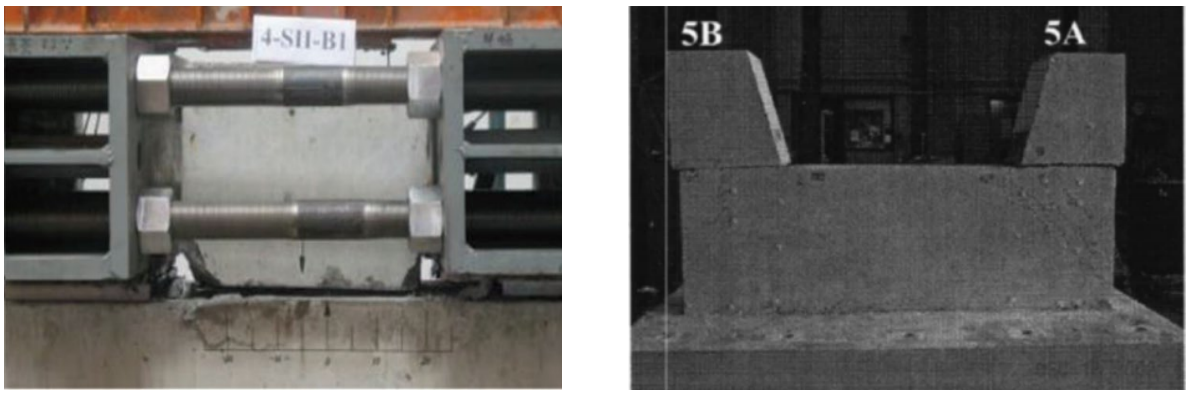

(a) Interior (Han *et al*., 2018) (b) Exterior (Bozorgzadeh *et al*., 2006)

Figure 1.7 Sliding friction failure mode of shear key

According to Yuan and Chen (2018), a smart shear key is designed to have a sliding friction failure mode, as shown in Figure 1.8. As a result, the bent cap or abutment will not be damaged due to the sacrifice of the shear key. After the earthquake, the shear key can be replaced conveniently. The typical failure mode is presented in Figure 1.9.

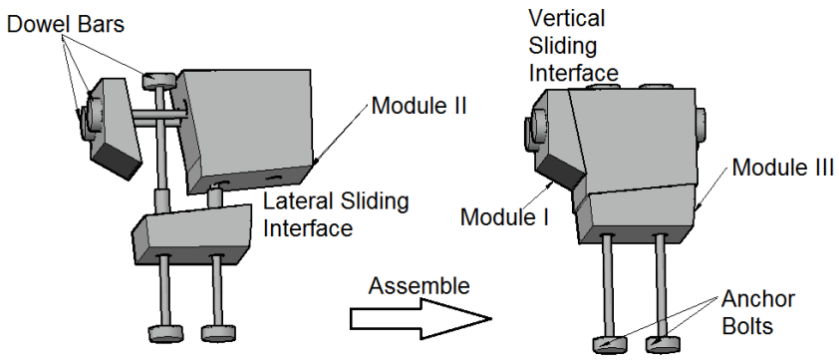

Figure 1.8 Assembling schematic of Smart shear keys

Figure 1.9 Failure mode of friction failure mode

1.3 OpenSEES model of shear key

The Open System for Earthquake Engineering Simulation (OpenSEES) software framework (Mazzoni *et al*., 2006) was developed and maintained by the Pacific Earthquake Engineering Research Center (PEER) and the George E. Brown Jr. Network for Earthquake Engineering Simulation (NEES). It has been widely adopted for seismic analysis of bridge structures due to its useful attributes like open-source, high computational efficiency, flexibility, and portability (McKenna, 2011). Many researchers in the past simulated the nonlinear behavior of bridge shear keys using OpenSEES, including but not limited to Abbasi and Moustafa (2017),

Goel and Chopra (2008), Omrani *et al*. (2017), Özşahin and Pekcan (2020), and Zaghi and Mehr (2018).

Özşahin and Pekcan (2020) studied the effect of torsional components of strong ground motions on the continuous concrete box-girder highway bridges with seat-type abutments. The authors simulated the bridge models in OpenSEES by considering the deck rotation that led to the contact between deck and shear keys. A shear key backbone developed by Megally *et al*., 2001 was built in the OpenSEES bridge model to capture the main characteristics like the yield force, yield, and ultimate deformations of the isolated shear keys. Nonlinear time history analysis (NLTHA) revealed the deck rotations are significantly amplified by the eccentricity of the deck touching the shear keys.

Zaghi and Mehr (2018) investigated the seismic performance of bridges with elastic and ductile shear keys. The authors conducted NLTHA of a set of one- to five-frame bridge structures with different geometries under thirty-three ground motions. The bridge models were simulated in OpenSEES. Two different types of shear key backbones, the elastic and elastic-perfectly-plastic force-displacement relationships, were considered and compared in the NLTHA. Three metrics were selected to evaluate these two shear keys, namely the maximum relative transverse displacement of frames, the residual relative displacement of adjacent frames, and displacement ductility demands on columns. It was concluded that limited yielding of in-span shear keys does not significantly affect the integrity of bridges.

Omrani *et al*. (2017) studied the seismic performance of a typical seat-type California bridge by considering its abutment backfill and shear-key models. Particularly, the inelastic force-displacement models of shear keys were used to account for the transverse response of bridge structures. Macro-elements of brittle and ductile shear keys were developed by combining

uniaxial material models in OpenSEES to generate the compression-only hysteretic force-displacement relationship. Their analyses revealed the coupling between the backfill and shear key responses is significant at moderate to large skew angles.

Abbasi and Moustafa (2017) investigated the seismic performance of regular and irregular bridges with and without shear keys. NLTHA was conducted in OpenSEES on three-dimensional numerical models of selected bridge configurations. An idealized trilinear force–deformation relationship was adopted to simulate the backbone of shear keys. The authors found that the impact of bridge shear keys depends on the bridge configuration and might significantly affect the irregular bridges. Meanwhile, shear keys played an important role in the moderate-level ground excitations.

Goel and Chopra (2008) examined the role of shear keys in the seismic performance of bridges. Three conditions, namely nonlinear shear keys, elastic shear keys, and no shear keys, were considered. Multiple bridge types without skew were simulated in OpenSEES by considering different span numbers (three spans vs. four spans) and symmetry variance. A simple trilinear force-deformation model was adopted to simulate the backbone of shear keys in this study. It was found that the seismic demands of bridges with nonlinear shear keys are generally bounded by the other two conditions. Thus, the upper and lower bounds of seismic demands of bridges crossing the fault-rupture zones are mainly determined by the cases of elastic shear keys and no shear keys.

Based on the above research, it could be seen that bridge shear keys are usually simulated by a simple trilinear force-deformation model when considering its nonlinearity and ductility.

Chapter 2 Performance of SMART Shear Key under Monotonic and Cyclic Loading

2.1 ABAQUS simulation platform

A smart shear key is designed as a joint to dissipate the energy induced by seismic or tsunami loading through friction between Modules I and II, Modules II and III, and Module II and dowel bar. The ABAQUS simulation platform is highly efficient at solving the nonlinear friction problems, and is used in this chapter to analyze the contact behavior between parts of the SMART shear key.

ABAQUS/Standard (implicit) and ABAQUS/Explicit can solve a wide variety of problems. In the simulation of SMART shear keys, the keys are slowly pushed horizontally, which represents a typical quasi-static problem. ABAQUS/Explicit is chosen in this study because the explicit method is more suitable for solving certain types of static problems than ABAQUS/Standard. One advantage of the explicit procedure is its ability to resolve complicated contact problems with greater ease (ABAQUS, 2014). To apply the explicit method to quasi-static problems, some special considerations are required. A static solution is always a time-consuming solution which is computationally impractical in its natural time scale. Therefore, to obtain an economical solution, the explicit analysis should model the process in a short time in which inertial forces remain insignificant.

2.2 Material properties

Modules I and III will adopt steel instead of concrete, considering the potential failure of these two parts that may result in the complete failure of the shear key. For Module II, the high-strength fiber concrete will be used in this study. Concrete damaged plasticity is used in this simulation to model concrete behavior. Compressive and tensile strengths of concrete are

considered to be 60 MPa and 2 MPa, respectively. The other material properties of concrete are shown below:

Table 2.1 Material properties used in the ABAQUS simulation

Dilation Angle	Eccentricity	fb0/fc0	K	Viscosity Parameter
30	0.1	1.16	0.6667	10^{-5}

To capture the nonlinearity of steel, it is modeled with an elastic-perfectly plastic material law given the grade of the rebars. The yield strength and elastic modulus of rebars are evaluated to be 450 MPa and 209 GPa, respectively.

2.3 Assembly and mesh

As shown in Figure 2.1, a SMART shear key consists of three modules, namely module I, module II, and module III, in addition to horizontal and vertical rebars. The sliding surface of module II is an inclined plane with an inclination of 5% between modules I and III, as shown in Figure 2.2. The steel rebars with diameters of 15.8 mm, 19.1 mm, and 22.2 mm are covered by plastic tubes with a diameter of 25 mm, which produced an interface between the rebar and concrete to eliminate the bond behavior and potential bond failure in practice. The width of the shear key was 200 mm. The thinnest part in modules I and III are 45.3 mm and 52.9 mm, respectively.

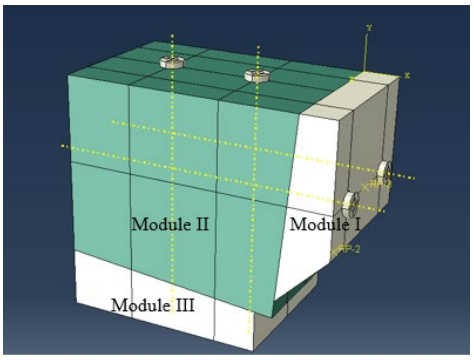

Figure 2.1 Assembly of smart shear key

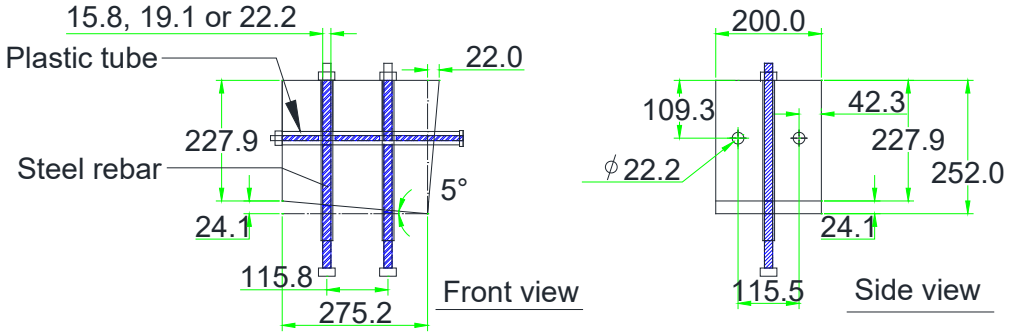

Figure 2.2 Schematic diagram of Module II of smart shear key (Unit: mm)

The meshing of a SMART shear key is shown in Figure 2.3. The element size for concrete and rebar are 10 mm×10 mm×10 mm and 10 mm×5 mm×5 mm, respectively.

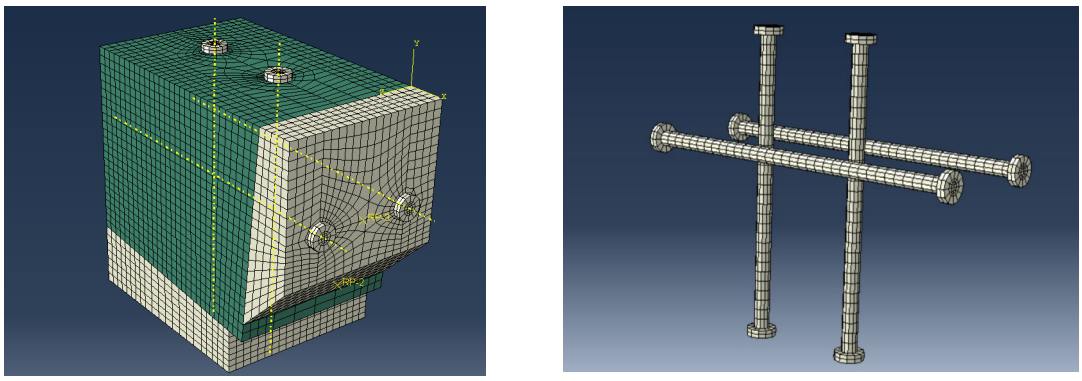

(a) Module I, II and III (b) Steel rebar

Figure 2.3 Meshing of smart shear key

2.4 Contact

The simulation of the SMART shear keys involves contact between different components like the bearing plates and concrete modules, between dowel bars and concrete modules, between concrete modules II and III, etc. There is a force normal to the contact point of the dowel bars and concrete modules. In the contact between the concrete Module II and Module III, there is friction between the surfaces, such that shear forces are created to resist the sliding of the bodies. The general goal of contact simulations is to find the contact areas and calculate the contact pressures. The friction coefficient between two concrete Modules is 0.41 based on the experimental results.

2.5 Load procedure

Two types of loads are applied on the smart shear key, which are horizontally monotonic loading and repeated loading.

2.6 Validation of finite element model

The former test result is used for validating the finite element model established in this study. The result was compared in Figure 2.4. It can be found that the experimental and numerical results agree well, indicating the parameters and modelling method used in this study are reasonably accurate.

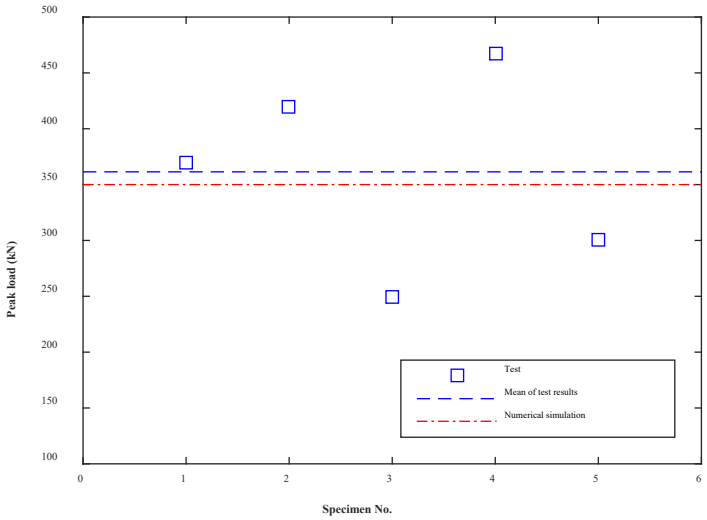

Figure 2.4 Comparison of force-displacement curves between experimental and numerical results

2.7 Results and discussions for monotonic loading

2.7.1 Failure mode

When the friction coefficient is 0.5, prestress on rebar is 200 MPa, and monotonic displacement is 50 mm, the typical failure mode of a SMART shear key under horizontal monotonic load shown in Figure 2.5 occurs. The figure depicts the departure between modules II and III, yielding and necking of vertical rebars, and tensile failure of concrete at the corner of module III.

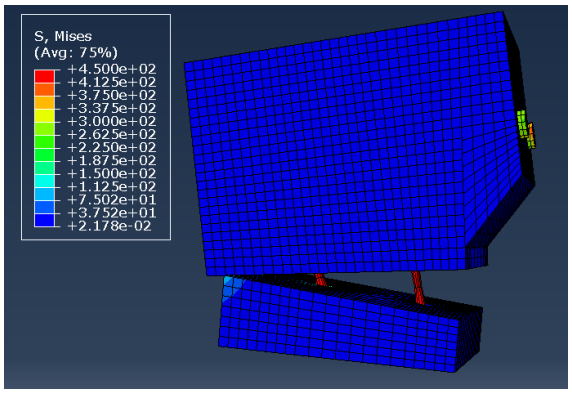

Figure 2.5 Typical failure mode of smart shear key under horizontal monotonic load

2.7.2 Parametric analysis

Three parameters, including prestress level, friction coefficient, and diameter of prestressing rebar, were investigated in this section.

2.7.2.1 Effect of prestress level

As shown in Figure 2.6, the load-displacement curve of the model shows that the SMART shear key works in three phases: slide, contact, and yield. First, the shear key module slides over some distance before the gap between the concrete module and steel anchor bars is closed. Due to friction between the concrete module and the steel module, some nonlinear effects are reflected in the force-displacement relation. Soon after the gap has been closed, the steel bars start to kink and yield rapidly. Even so, the shear key can still resist the applied load to a large displacement due to the excellent ductility of the steel bars. The increase in prestress level leads to a significant improvement in initial stiffness but has little effect on the post-peak behavior. The load-displacement behavior is similar to the theoretical model proposed by Silva *et al.* (2009), as demonstrated in Figure 2.7.

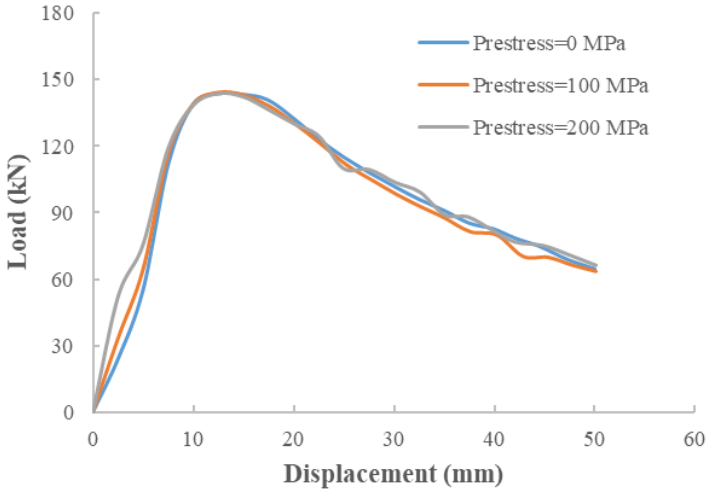

Figure 2.6 Load versus displacement curve under different prestress level

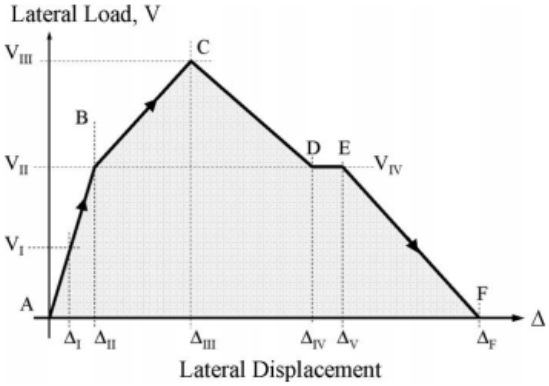

Figure 2.7 Hysteresis rule for exterior shear keys (Silva *et al*., 2009)

2.7.2.2 Effect of friction coefficient

With an increased friction coefficient, the initial stiffness increases correspondingly; the load capacity increases but with a decreasing slip, as depicted in Figure 2.8. After the peak, the curve shows a little bit of fluctuation due to the unstable movement of the concrete modules as well as the iteration algorithm.

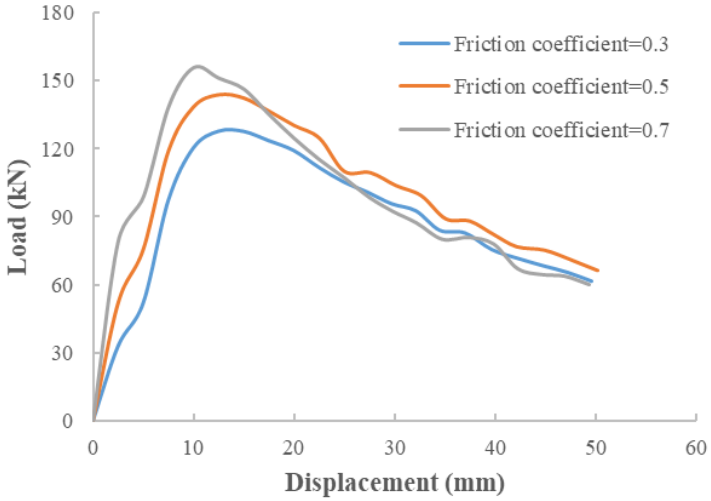

Figure 2.8 Load versus displacement curve with different friction coefficient

2.7.2.3 Effect of diameter of prestressing bar

The load-displacement behavior with variations in the diameter of prestressing rebar is presented in Figure 2.9. It can be found that both the initial stiffness and load capacity increase with the increase in diameter of the rebar, as expected. The load capacity increases more significantly than the friction coefficient.

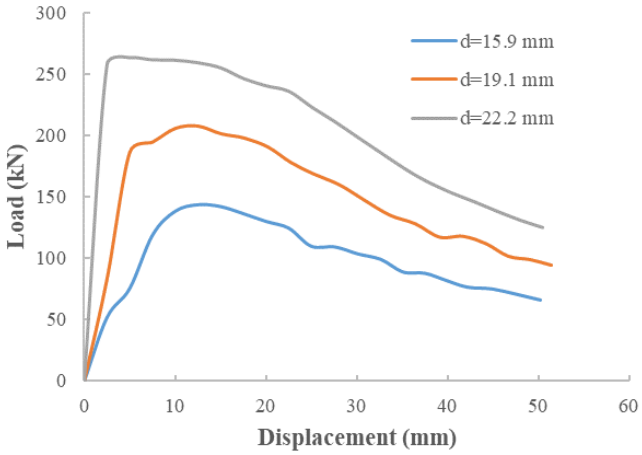

Figure 2.9 Load versus displacement curve with different diameter of rebar

2.7.3 Steel rebar response

The steel rebar and reaction load response time histories are shown in Figure 2.10. It can be found that the rebar does not yield when the reaction load reaches the peak load. The yield of the reaction load is due to the departure of the concrete modules.

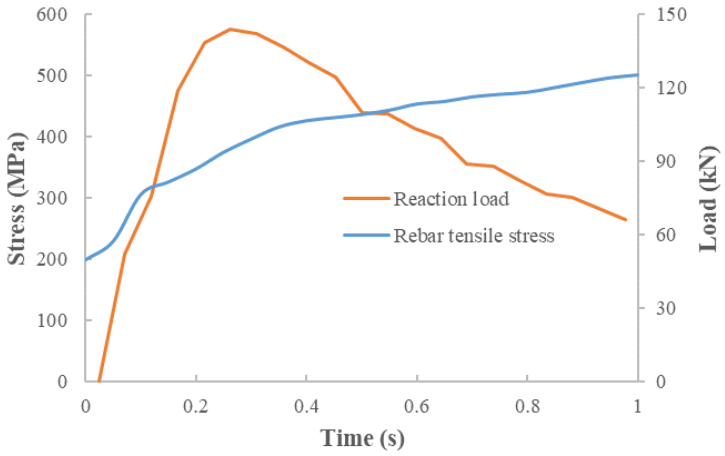

Figure 2.10 Steel rebar and reaction load response times history

2.8 Results of repeated loading

The repeated loading applied on the SMART shear key is shown in Figure 2.11. The amplitudes of the peak load are 2.0 mm, 3.8 mm, 7.7 mm, and 14.7 mm. The diameter of the rebar is 15.9 mm, with the prestress level and friction coefficient of 200 MPa and 0.5, respectively.

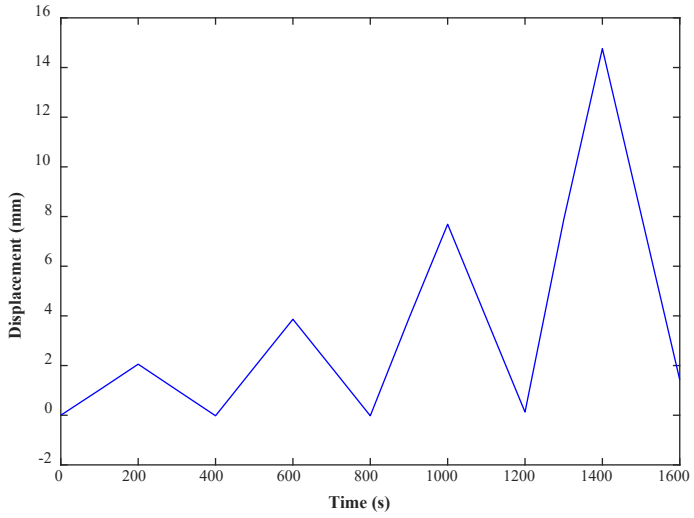

Figure 2.11 Displacement time history applied on the shear key

The load applied on the shear key is presented in Figure 2.12. The peak load increases with the displacement input at the beginning, but it falls to around 15 kN after the second peak. On the contrary, the load in the negative direction keeps a high level.

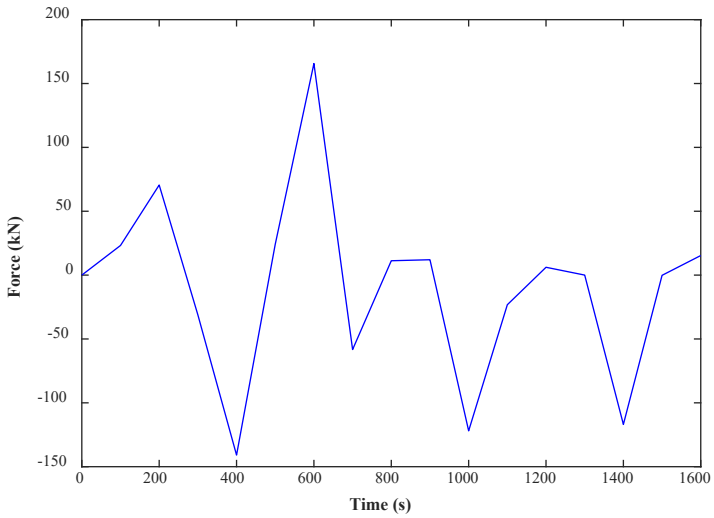

Figure 2.12 Force time history applied on the shear key

The load-displacement response of the shear key is shown in Figure 2.13. The hysteretic loop indicates the capability of the shear key for energy dissipation.

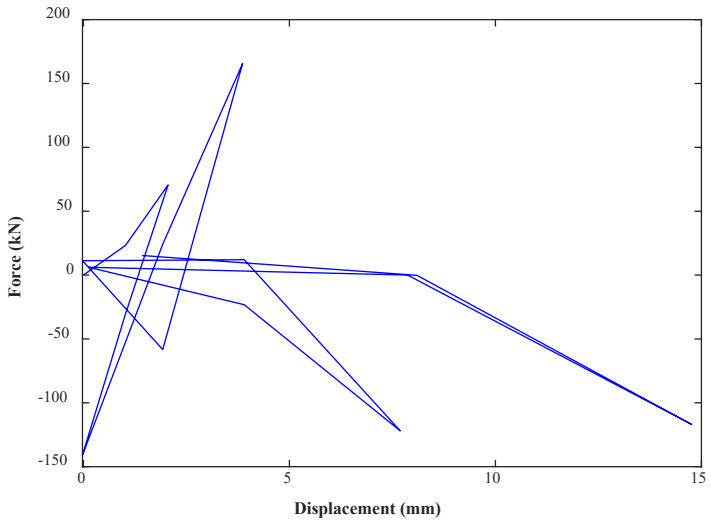

Figure 2.13 Load-displacement response of the SMART shear key under repeated loading

2.9 Summary

- The numerical simulation results indicate that the SMART shear key works in three phases: slide, contact, and yield. The shear key can resist the applied load to a large displacement due to the excellent ductility of the steel bars.
- The increase in prestress level leads to a significant improvement in initial stiffness but has little effect on the post-peak behavior.
- With the increase in the friction coefficient, the initial stiffness and load capacity increase correspondingly.

- Both initial stiffness and load capacity increase with the increase in diameter of the rebar, as expected. The load capacity increases more significantly than the friction coefficient.
- Under repeated loading, the hysteretic loop indicates the capability of the shear key for energy dissipation.

Chapter 3 Performance of a Bridge with SMART Shear Keys under Seismic Loading

3.1 Bridge introduction

Reinforced-concrete bridges in California typically consist of a multicell box girder deck supported on abutments at two ends and single or multiple intermediate bents. As shown in Figure 3.1, the abutment consists of two wing walls, a back wall, shear keys exterior, a seat, footing, and piles if needed. The shear keys at the abutment of bridges are designed to provide transverse restraint to the superstructure during service load and moderate earthquakes. During the maximum considered earthquake (MCE), however, the shear keys are designed to serve as sacrificial elements to protect the abutment stem wall, wing walls, and piles from damage, implying the shear keys will break off before damage occurs in piles or abutment walls.

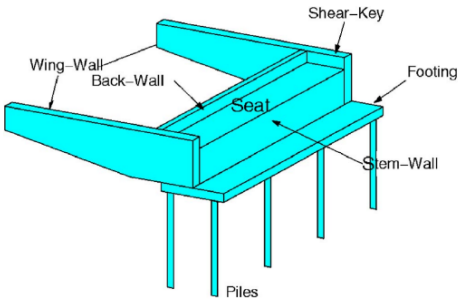

Figure 3.1 Typical abutment details (Goel and Chopra, 2008)

The 2006 California Department of Transportation (CALTRANS) seismic design criteria (SDC) for shear keys in ordinary bridges limit the capacity of shear keys to be smaller than 30% of the dead load vertical reaction at the abutment and 75% of the total lateral pile capacity (CALTRANS, 2006). However, this criterion was changed to be smaller than 50% of the dead

load vertical reaction at the abutment and 75% of the total lateral pile capacity plus one wing wall shear capacity in CALTRANS (2019).

The bent caps of the bridge support the continuous girders. The typical schematic view of the shear key on bent caps is presented in Figure 1.1 (b) and Figure 1.2 (b). Both interior and exterior shear keys can be installed on the bent cap.

The bridge deck is supported on the substructure by conventional bearings. Fixed bearings are located on cap beams, and sliding bearings are located at the abutments providing expansion joints at these locations. The bridge foundations consist of spread footing, piles, or pile shafts, with underlying soil that is not susceptible to liquefaction, lateral spreading, or scour.

3.2 Modeling

The selected bridge systems are analyzed using the structural analysis software Open System for Earthquakes Engineering Simulation OpenSees (McKenna, 2011). The superstructure is modeled as linearly elastic beam-column elements that follow the alignment of the bridge with line elements at the centroid of the cross-sections. In order to capture the distribution of mass along the length of the deck, nineteen elements with equal length segments per span are used. The schematic view of the bridge model is presented in Figure 3.2. The bridge is a continuous concrete bridge with three spans (Zhong *et al*., 2015), each span having a length of 38 m. The pier is 8 m in height. The longitudinal and volume steel ratios are 0.8% and 0.5%, respectively.

Since no damage or significant nonlinear behavior is expected within the superstructure and the foundation system, the superstructure elements, the cap beam, and the foundation springs are all considered as linear elastic elements.

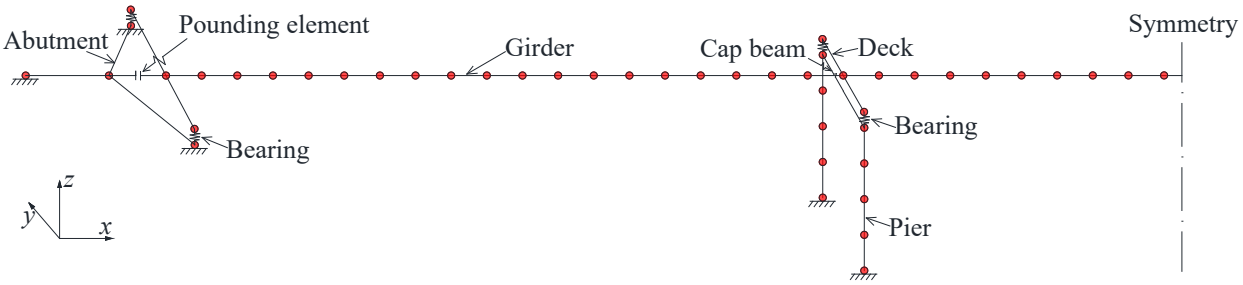

Figure 3.2 Bridge model

3.2.1 Pier and cap beam modeling

The columns will yield and suffer damage under strong ground motions, and therefore nonlinear beam-column elements are used to model the columns. The specified cross-sectional properties are based on a fiber section. All fiber sections are assigned with the UniaxialMaterial model tag of OpenSEES. Three constitutive rules pertaining to confined concrete, unconfined concrete, and steel rebar, are used to represent the given fiber material properties of the cross-section. Four force-based beam-column elements are used to simulate the nonlinear behavior of each column. The profile of the pier is square, with a dimension of 1.7 m×1.7 m×8 m. The steel rebar is of HRB 335 level. The concrete type is C40. Steel02 and Concrete01 are used to simulate the steel rebar and concrete behavior, respectively.

To model the bent cap, a rigid element is attached to the top of the columns. The length of this rigid element is set equal to the length of the bent cap. The rigid element has the same six freedom degree movement as the adjacent nodes on the bridge deck.

3.2.2 Bearing

Elastomeric Bearing Pads (Neoprene pad) bearings are adopted for supporting the bridge girders on piers as fixed bearings. Polytetrafluoroethylene (PTFE) is used for supporting girders on abutments as a sliding bearing. The initial stiffnesses for these two types of bearings are

4.5×10^4 kN/m and 1.9×10^4 kN/m, respectively. The yield strengths for these bearings are 1177 kN and 1900 kN, respectively. Steel01 and ElasticPP models are respectively adopted for simulating the horizontal constitutive behaviors, as shown in Figure 3.3 (a) and (b), respectively. The vertical stiffness is recognized to be unlimited.

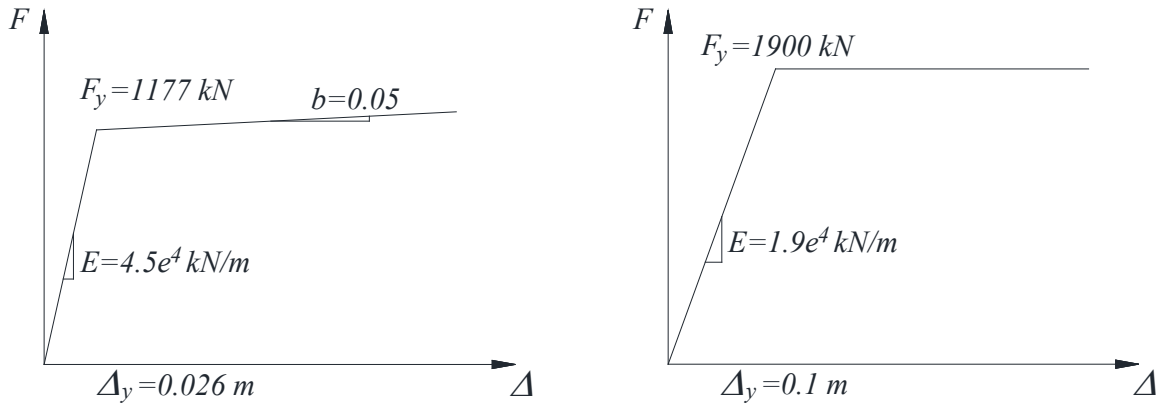

(a) Neoprene pad bearing (b) PTFE bearing

Figure 3.3 Constitutive relationship of bearing in vertical direction

3.2.3 Abutment

The abutment is modeled with a weightless rigid element of length equal to the superstructure width, connected through a rigid joint to the superstructure centerline. The nonlinear behavior of the abutments is modeled as springs in the longitudinal directions, which are elastic-perfectly plastic springs with a gap to account for the gap between the end of the deck and the abutment back wall. The constitutive relationship of the pond effect is shown in Figure 3.4.

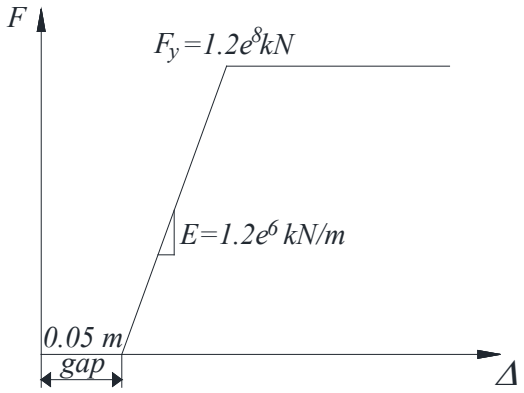

Figure 3.4 Constitutive behavior of abutment in longitudinal direction

3.2.4 Shear key

The transverse springs are used to simulate the contributions of the shear keys. The locations of the mid-span and abutment shear keys are shown in Figure 3.5. Three cases with three statuses of shear key are analyzed. The first case is when no shear key is applied in the model, as shown in Figure 3.2. The second one involves applying shear keys in the mid-span, and a total of four shear keys are adopted in the model. The last one entails employing shear keys in both the mid-span and abutment areas, and a total of eight shear keys are used.

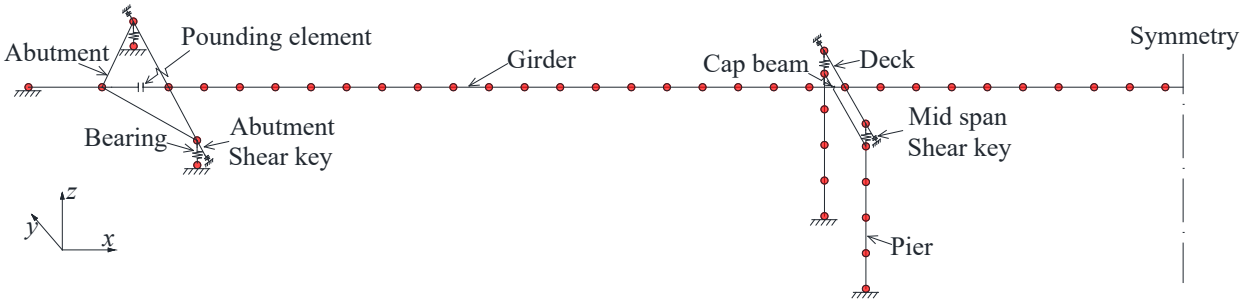

Figure 3.5 Bridge model with shear keys

Since no consensus has yet been reached on the force-deformation (or hysteretic) behavior of shear keys, this investigation utilizes a simple trilinear force-deformation model based on the experimental results obtained from the authors' previous research on shear keys (Chen and Yuan, 2017). The constitutive relationship of the shear key is presented in Figure 3.6. The zero-length elements with uniaxial behavior, whose properties are discussed later, are distributed along the cap beam and abutment to model the transverse reactions by the shear keys.

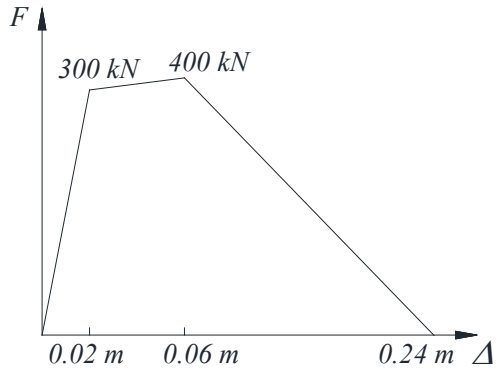

Figure 3.6 Force-deformation behavior of shear keys and abutment

3.3 Performance of shear key under earthquake loading

The 1989 Loma Prieta earthquake wave with a PGA of 0.8 g is adopted in this study, as shown in Figure 3.7. This wave is uniformly applied to the base of the bridge in the transverse direction.

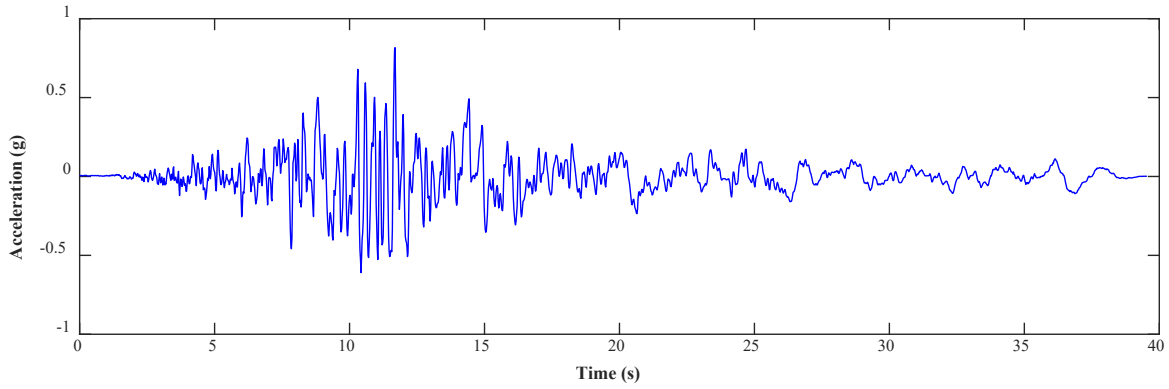

Figure 3.7 Acceleration input for simulation

3.3.1 Displacement performance

The displacement of the pier column drift is presented in Figure 3.8 (a). It can be found that the shear keys added in the mid-span or all spans can significantly limit the pier column drift in the mid-span. This is due to energy dissipation by the shear key. However, it seems that no significant difference can be found by using a mid-span shear key or an all-span shear key. A similar result can also be found in the deck displacement at the abutment, as shown in Figure 3.8(b). Adding an all-span shear key led to a slightly lower displacement than that caused by adding a mid-span shear key, which is along the expected lines.

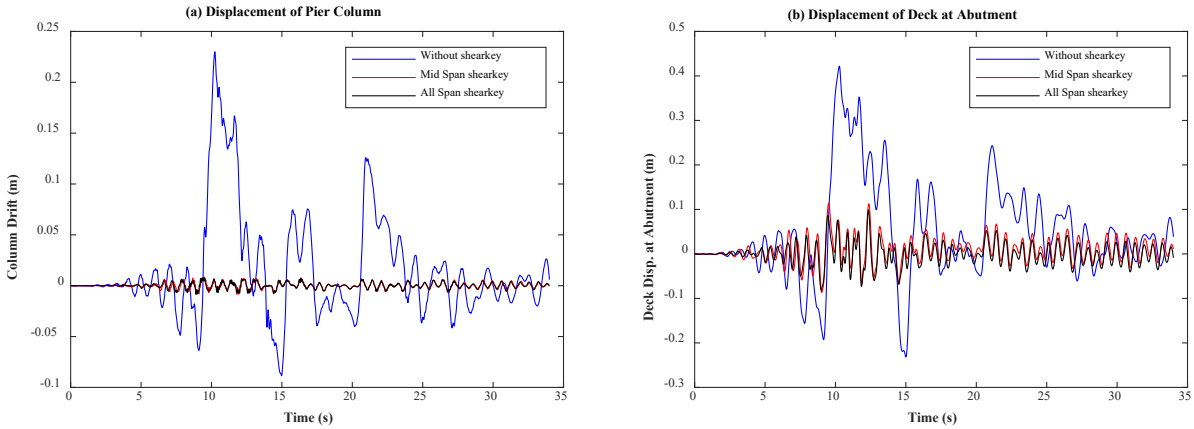

Figure 3.8 Displacement-time history of pier column and deck at abutment

As shown in Figure 3.9, the displacement of bearing in the mid-span is greatly reduced after adding the shear keys. The displacement of bearing in the middle span is smaller after adding an all-span shear key than after adding a mid-span shear key only.

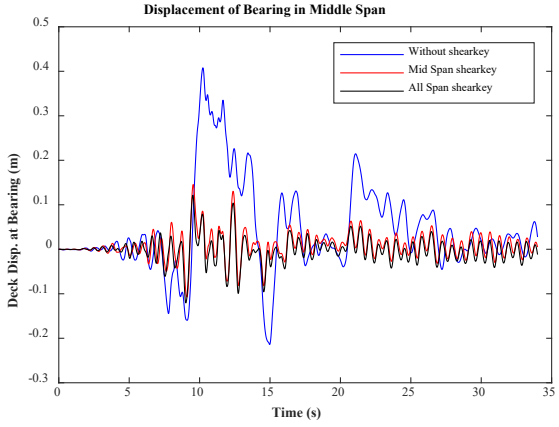

Figure 3.9 Displacement-time history of deck at bearing in middle span

3.3.2 Load performance

As shown in Figure 3.10 (a), the force of the pier column is reduced slightly after adding shear keys at the mid-span or all spans. As presented in Figure 3.10 (b), the force on the deck at the abutment greatly increases after adding a mid-span shear key, indicating the force is transferred from mid-span to the abutment. After adding all span shear keys, the force on the deck at the abutment is reduced. This means the shear key can optimize the force distribution between the mid-span and the abutment.

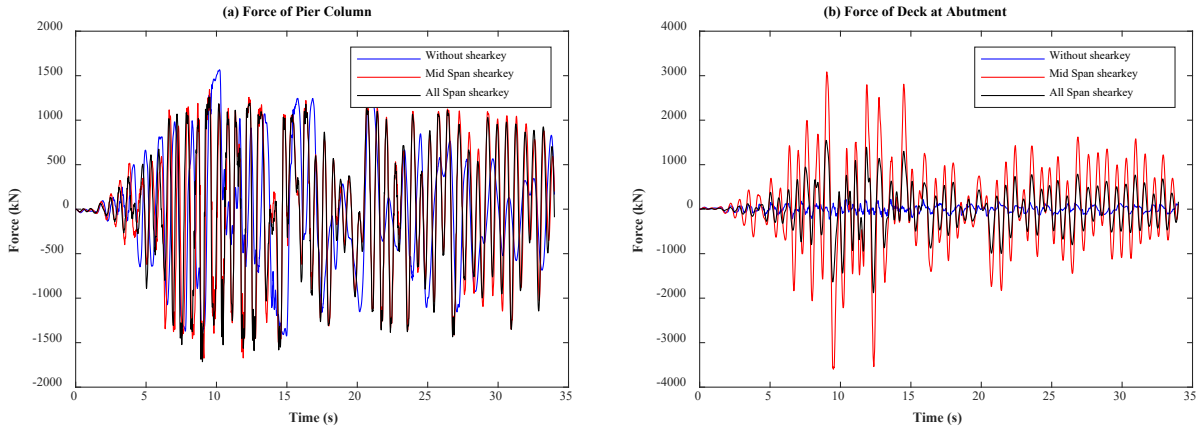

Figure 3.10 Force-time history of pier column and deck at abutment

As shown in Figure 3.11, the force of bearing in the middle span does not change significantly after adding mid-span or all span shear keys. This may be due to the relatively low yield strength of the bearing.

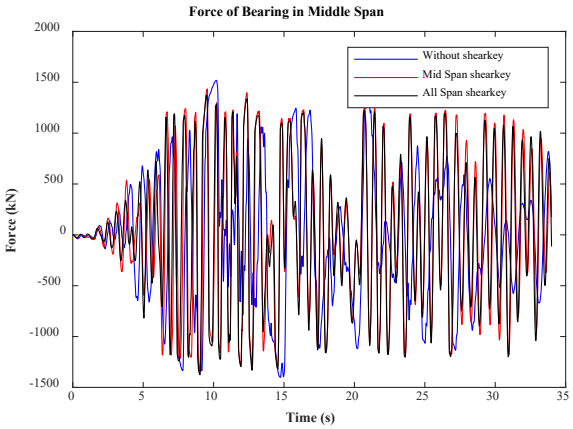

Figure 3.11 Force-time history of bearing in middle span

3.3.3 Hysteretic performance

3.3.3.1 Shear key

The hysteretic behavior of the shear key at the mid-span is shown in Figure 3.12 (a). It can be found there is greater displacement even after adding all span shear keys compared with only adding a mid-span shear key. This indicates the shear key should be added to all spans to optimize the displacement response of the shear key as well as the bridge deck, as mentioned before. The shear key yields due to the strong earthquake loading. The hysteretic curve is full, indicating the shear key can be used to dissipate the energy induced by a seismic event. The shear key at the abutment also yields, as shown in Figure 3.12 (b), even though the displacement is less than that at the mid-span. This can be attributed to the higher stiffness and yield strength of bearing at the abutment.

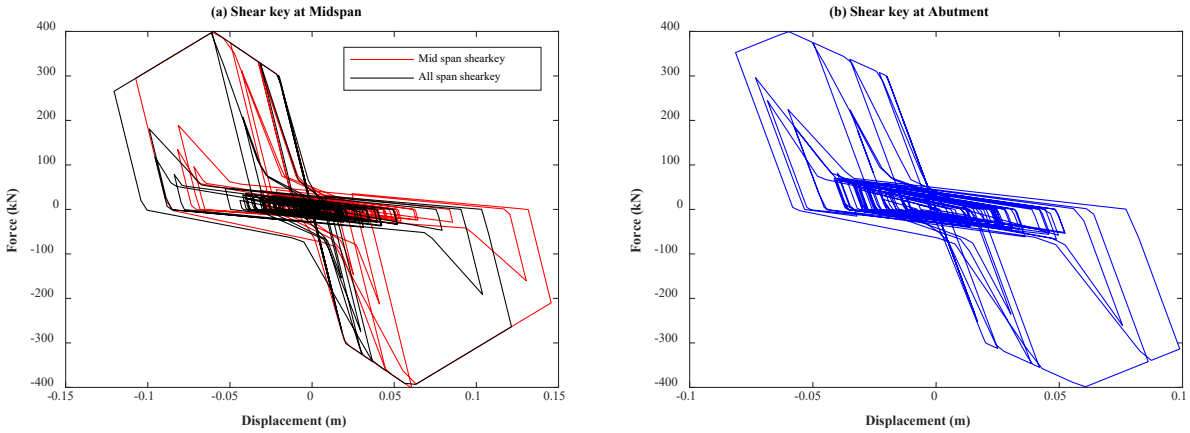

Figure 3.12 Hysteretic response of shear key at mid span or abutment

3.3.3.2 Bearing

The response of the bearings is presented in Figure 3.13. As shown in Figure 3.13 (a), it can be found there is a greater displacement response of the bearing at the mid-span even after adding all span shear keys compared with adding a mid-span shear key. The bearing is still in the linear stage when all-span shear keys are applied, as shown in Figure 3.13 (b). However, the shear key is in the nonlinear stage when only a mid-span shear key is added. This indicates shear keys should be added to all spans to get an optimal displacement and force response.

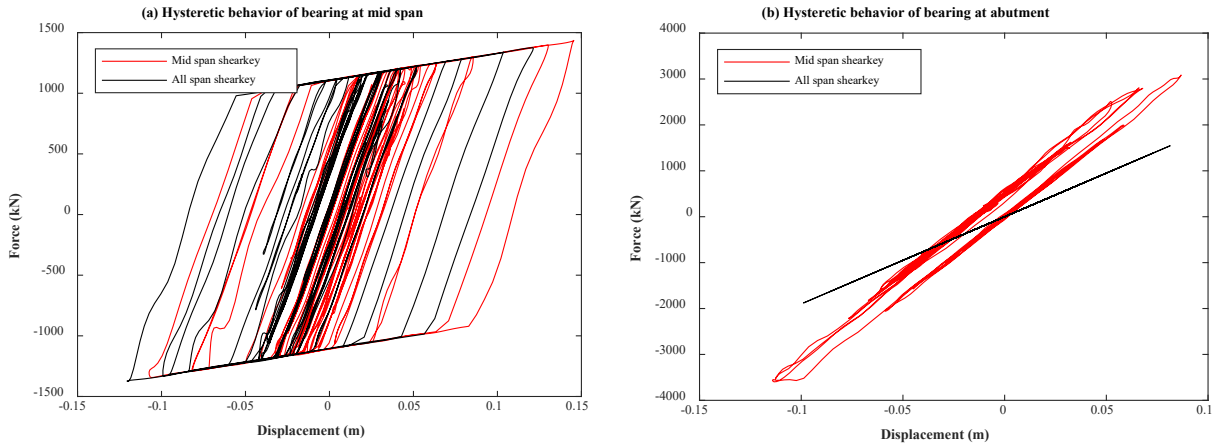

Figure 3.13 Hysteretic response of bearing at mid span or abutment

3.4 Summary

- SMART shear keys added in the mid-span or all spans can significantly limit the pier column drift in the mid span, due to their capability of energy dissipation. Similar results can also be found in the deck displacement and bearing displacement at the mid-span.
- The force of the pier and bearing in the middle span does not change significantly after adding mid-span or all-span shear keys, which is attributable to the relatively low yield strength of the bearing.
- The force on the deck at the abutment greatly increases after adding a mid-span shear key, indicating the force is transferred from the mid-span to the abutment. After adding all-span shear keys, the force on the deck at the abutment is reduced. This means that the shear key can optimize the force distribution between the mid-span and the abutment.
- The displacement of the shear key in the mid-span is higher even after adding all-span shear keys compared with only adding a mid-span shear key, indicating the shear key

should be added to all spans to optimize the displacement response of the shear keys as well as the bridge deck.

- The displacement response of the bearing at the mid-span is higher even after adding all-span shear keys compared with adding a mid-span shear key. The bearing at the abutment is still in the linear stage when all-span shear keys are applied. However, the shear key is in the nonlinear stage when only a mid-span shear key is added. This indicates the shear key should be added to all spans to strike a balance between the displacement and force responses.

References

Abbasi, M., & Moustafa, M. A. 2017. Effect of shear keys on seismic response of irregular bridge configurations. Transportation Research Record. https://doi.org/10.3141/2642-17.

ABAQUS/Standard User's Manual. 2014. Version 6.14. Providence, Dassault Systèmes Simulia Corp.

Bozorgzadeh, A., Megally, S., Restrepo José, I., & Ashford Scott, A. 2006. Capacity Evaluation of Exterior Sacrificial Shear Keys of Bridge Abutments. *Journal of Bridge Engineering*, *11*(5), 555–565. https://doi.org/10.1061/(ASCE)1084-0702(2006)11:5(555).

Caltrans. 2006. Seismic Design Criteria, Version 1.4, *California Department of Transportation*, *Sacramento*, CA.

Caltrans. 2019. Seismic Design Criteria, Version 2.0, *California Department of Transportation, Sacramento*, CA.

Chen G., & Yuan X. 2017. *Design and Study of a Novel SMART Bridge Shear Key for Earthquake and Tsunami Hazards Mitigation*. Mid-America Transportation Center.

Goel, R. K., & Chopra, A. K. 2008. Role of Shear Keys in Seismic Behavior of Bridges Crossing Fault-Rupture Zones. Journal of Bridge Engineering. *13*(4), 398–408. https://doi.org/10.1061/(asce)1084-0702(2008)13:4(398).

Han, Q., Hu, M.-H., Wen, J.-N., & Du, X.-L. 2020. Seismic Capacity Evaluation of Interior Shear Keys for Highway Bridges. *Journal of Earthquake Engineering*, *24*(6), 972–987. https://www.tandfonline.com/doi/abs/10.1080/13632469.2018.1453414.

Han, Q., Hu, M.-H., Zhou, Y.-L., & Du, X.-L. 2018. Seismic Performance of Interior Shear Keys of Highway Bridges. *ACI Structural Journal*, *115*(4), 1011–1021. https://www.concrete.org/publications/internationalconcreteabstractsportal/m/details/id/51701916.

Han, Q., Zhou, Y., Ou, Y., & Du, X. 2017. Seismic behavior of reinforced concrete sacrificial exterior shear keys of highway bridges. *Engineering Structures*, *139*, 59–70. https://doi.org/https://doi.org/10.1016/j.engstruct.2017.02.034.

Kottari, A., Shing, P. B., & Bromenschenkel, R. 2020. Shear Behavior of Exterior Non-Isolated Shear Keys in Bridge Abutments. *ACI Structural Journal*, *117*(2), 225–237. https://www.concrete.org/publications/internationalconcreteabstractsportal.aspx?m=details&id=51721317.

Mazzoni, S., McKenna, F., Scott, M. H., & Fenves, G. L. 2006. OpenSees command language manual. Pacific Earthquake Engineering Research Center.

McKenna, F. (2011). OpenSees: A framework for earthquake engineering simulation. Computing in Science and Engineering. https://doi.org/10.1109/MCSE.2011.66.

Megally, S., Silva, P., & Seible, F. 2001. *Seismic Response of Sacrificial Shear Keys in Bridge Abutments*. UCSD/SSRP-2001/23, University of California, San Diego. Department of Structural Engineering.

Omrani, R., Mobasher, B., Sheikhakbari, S., Zareian, F., & Taciroglu, E. 2017. Variability in the predicted seismic performance of a typical seat-type California bridge due to epistemic uncertainties in its abutment backfill and shear-key models. Engineering Structures. *148*, 718–738. https://doi.org/10.1016/j.engstruct.2017.07.018.

Özşahin, E., & Pekcan, G. 2020. Inelastic seismic response of box-girder bridges due to torsional ground motions. Engineering Structures. *218*, 110831. https://doi.org/10.1016/j.engstruct.2020.110831.

Silva, P. F., Megally, S., & Seible, F. 2009. Seismic performance of sacrificial exterior shear keys in bridge abutments. *Earthquake Spectra*, *25*(3), 643–664. https://journals.sagepub.com/doi/abs/10.1193/1.3155405.

Silva, P. F., & Nguyen, T. L. T. 2010. Influence of shear key modeling on the performance of bridges under simulated seismic loads. Bridge Maintenance, Safety, Management and Life-Cycle Optimization - Proceedings of the 5th International Conference on Bridge Maintenance, Safety and Management. https://doi.org/10.1201/b10430-364.

Yuan, X., & Chen G., An Adaptive SMART Shear Key and its Mechanical Properties for Earthquake/Tsunami Mitigation, Proceedings of the 7th World Conference on Structural Control and Monitoring (2018, Qingdao, China), International Association for Structural Control and Monitoring (IASCM), Jul 2018.

Zaghi, A. E., & Mehr, M. 2018. Elastic versus ductile seismic design concept for shear keys in in-span hinges of multi-frame bridges. 11th National Conference on Earthquake Engineering 2018, NCEE 2018: Integrating Science, Engineering, and Policy.

Zhong, J., Pang, Y., Cao, S., & Yuan, W. 2015. Seismic fragility methodology for RC continuous bridges based on components correlation, *Journal of Tongji University (Natural Science), 43*(2), 193-198.